



HAL
open science

Dependence, on the Cr Content, of the Corrosion Resistance to Fusayama Saliva of Cobalt-Based Dental Alloys, Studied by the Mean of Binary Alloys

Patrice Berthod, Estelle Kretz

► **To cite this version:**

Patrice Berthod, Estelle Kretz. Dependence, on the Cr Content, of the Corrosion Resistance to Fusayama Saliva of Cobalt-Based Dental Alloys, Studied by the Mean of Binary Alloys. *ES Journal of Dental Sciences*, 2020, 1. hal-02495046

HAL Id: hal-02495046

<https://hal.science/hal-02495046>

Submitted on 29 Feb 2020

HAL is a multi-disciplinary open access archive for the deposit and dissemination of scientific research documents, whether they are published or not. The documents may come from teaching and research institutions in France or abroad, or from public or private research centers.

L'archive ouverte pluridisciplinaire **HAL**, est destinée au dépôt et à la diffusion de documents scientifiques de niveau recherche, publiés ou non, émanant des établissements d'enseignement et de recherche français ou étrangers, des laboratoires publics ou privés.

Dependence, on the Cr Content, of the Corrosion Resistance to Fusayama Saliva of Cobalt-Based Dental Alloys, Studied by the Mean of Binary Alloys

Research article

Patrice Berthod^{1,2*} and Estelle Kretz²

¹Institut Jean Lamour, University of Lorraine, France

²Faculty of Science and Technologies, Vandoeuvre-lès-Nancy Cedex, France

Received: Jan 14, 2020; **Accepted:** Jan 29, 2020; **Published:** Feb 12, 2020

***Corresponding author:** Patrice Berthod, Institut Jean Lamour, Faculty of Science and Technologies, Campus Victor Grignard, P.B. 70239, 54506 Vandoeuvre-lès-Nancy Cedex, France

Copyright: © 2020 Patrice Berthod. This is an open-access article distributed under the terms of the Creative Commons Attribution License, which permits unrestricted use, distribution, and reproduction in any medium, provided the original author and source are credited.

Abstract

Cobalt-chromium alloys represent a growing alternative for dental alloys made of noble metals. Superior mechanical strength and the development of a passive layer allow them resisting mastication and aggressiveness of the buccal milieu, respectively. However the Cr content merits to be optimized for achieving fabrication easiness, corrosion resistance and ductility keeping. This work consists in a specific analysis of the dependence of the properties of cobalt-chromium alloys on their Cr contents. To eliminate the possible influences of a maximum of other factors simple binary alloys were initially prepared all according to a precise procedure leading to equi-axed polycrystalline single-phased alloys, chemically homogeneous and with the same mechanical internal states. In parallel with controls in chemical composition, microstructure and hardness, all of them were subjected to electrochemical characterization of corrosion with the same apparatus and the same protocol: Fusayama saliva acidified to pH=2.3, 37±0.5°C, and successive classical electrochemical tests with the same parameters: free potential following up, Stern-Geary method, Tafel method. Results demonstrate that high corrosion resistance thanks to passivation is systematic for Cr content equal or higher than 25wt. %, that 20 wt. %Cr may lead to not reproducible behavior, and lower contents allow high corrosion rates.

Keywords

Biomaterials; Oral and maxillofacial; Prostheses; Cobalt-chromium dental alloys; Acidic Fusayama artificial saliva; Corrosion

Introduction

Alloys made of noble metals are used for many years for various types of dental prostheses. One of these applications is the metallic framework which reinforces mechanically fixed partial denture to allow them resisting the high stresses induced by mastication. They are generally not visible because they are covered by the cosmetic ceramics looking like natural teeth [1]. These metallic frameworks are not monolithic but composed of major parts of parent alloys joined together by soldering. Until fairly recently

these parent alloys were more or less rich in noble metals (palladium, gold, platinum). The sum of weight contents of these elements may represent more than 25wt.% ("Noble" alloys) and even more than 60wt.% ("High Noble" alloys). Such alloys are logically costly and it is tried, from several decades, to replace them by much cheaper alloys base on nickel or on cobalt, elements intrinsically strong enough to resist mastication-induced stresses, and even to resist creep deformation in totally different applications, as base elements for superalloys suitable to high temperature uses

[2,3]. In this last applications nickel and cobalt are alloyed with aluminum or chromium to resist both oxidation by hot gases and corrosion by molten substances [4].

These two elements presenting the particularity to induce the development of a continuous external protective oxide. In situation of corrosion at ambient or body temperature the same elements are useful for protecting the alloys but the formed passivation scale are much thinner than what is observed at elevated temperature. Unfortunately aluminum and nickel may threaten health [5] by inducing possible diseases or allergy problems [6] that chromium and cobalt [7] do not.

Cobalt-chromium is considered as the base of many cobalt-based alloys [8], beside other dental cobalt alloys involving also noble elements (e.g. Au [9]) or other ones (e.g. Ti [10-12]). Other elements can be also found in the chemical compositions of dental cobalt-chromium alloys such as tungsten [13,14], molybdenum [15,16], tantalum [17], niobium and even ruthenium [18,19]. Unlike nickel-based dental alloys, only few studies were devoted to a good knowledge and comprehensiveness of the behavior of dental cobalt alloys in corrosion in the buccal milieu [20].

A good resistance of dental alloys of the Predominantly Base category, cast {cobalt & chromium}-based alloys for instance, against possible corrosion on long time in mouth is compulsory. This may be achieved by choosing chromium contents high enough to be sure to obtain and maintain the passivation layer for almost stopping possible corrosion. However the Cr content must be not too high to avoid any precipitation of brittle phases at solidification. Furthermore, it can be interesting to decrease the chromium content to lower the difficulties of melting due to this rather refractory element (fusion point of Cr: 1870°C, against 1495°C for Co). An optimized Cr content allowing a good compromise between easiness fabrication by casting

and corrosion resistance may be very useful to know. This is precisely the purpose of the present work. This one aims to work on a common base to many cobalt-based dental alloys, constituting of the binary cobalt-chromium system. To do that a series of binary alloys was elaborated by foundry. Their Cr content varied from 0 (pure cobalt) to a maximum of 30 wt.%Cr, by slices of 5 wt.%. The ductility of these seven materials at room temperature, which depends on the Cr content, was assessed indirectly through indentation tests and their corrosion behaviors were explored by using a milieu simulating human saliva and methods conventionally used elsewhere to specify the behavior of metallic materials in liquids.

Materials and methods

Elaboration

Obtaining the alloys to study was realized by melting pure parts of cobalt and of chromium together in the fusion chamber of a furnace (CELES, France). The pure elements (> 99.9%) were bought by Alfa Aesar and the received small parts were weighed using precision balance to constitute the charges, targeting a total of about 40 grams. These parts were placed in the copper crucible of the furnace. By considering the high reactivity at elevated temperature of both elements especially chromium), an

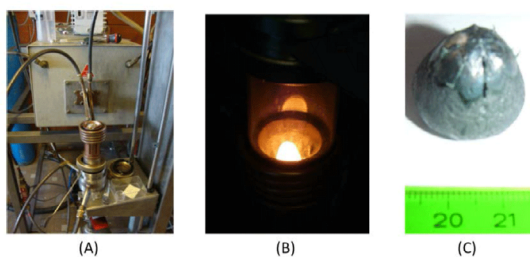


Figure 1: Preparation of the alloys: cobalt and chromium parts placed in the copper crucible (A), liquid alloy at the stage of isothermal homogenization (B) and the obtained ingot (C)

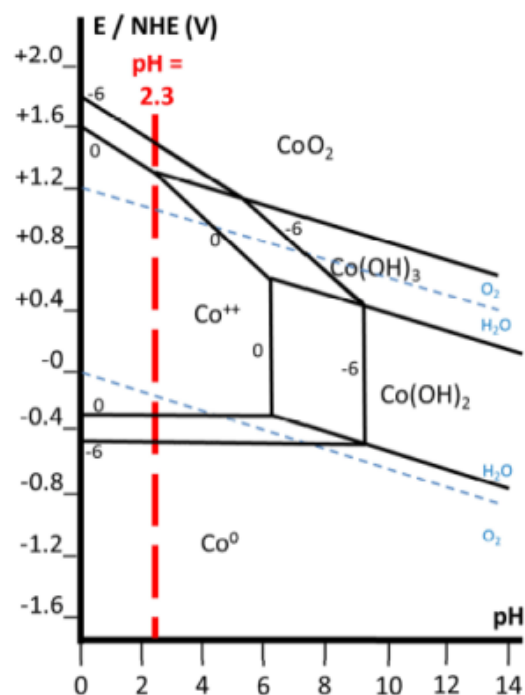


Figure 2: Simplified Pourbaix diagram of cobalt

Table 1: Composition of the artificial saliva prepared for the study (Fusayama, acidified to pH=2.3)

Species	Provider	Purity (%)	Concentration in saliva (g/L)
KCl	Carl Roth	≥ 99	0.4
NaCl	AnalaR Normapur®	≥ 99.5	0.4
CaCl ₂ , 2H ₂ O	Sigma-Aldrich	≥ 99	0.906
NaH ₂ PO ₄ , 2H ₂ O	Sigma-Aldrich	≥ 99	0.69
(NH ₂) ₂ CO	Carl Roth	≥ 99.5	1
Na ₂ S, 9H ₂ O	Alfa Aesar	≥ 98	0.005

inert atmosphere was created around these metals for all the heating, melting and cooling. For that a silica tube was placed around the crucible, closed and pumping was applied to decrease the internal pressure down to 5×10^{-2} millibars. After that, pure Argon was introduced inside until reaching again about 800 millibars. New pumping followed by new pure Ar introduction, was repeated two times. Finally, the obtained internal atmosphere was constituted of 400 millibars of pure argon, with the same contents in residual gases as in the Argon of the bottle, thanks to this triple dilution.

Thanks to a copper coil surrounding the external face of the silica tube, a intense alternative magnetic field was generated by the circulation of an alternative electric current (frequency: between 100 and 110 kHz, applied voltage: 4 kV). By progressively increasing the provided power, heating of the Co parts and of the Cr parts led to their melting and their mixing. After about five minutes spent in the liquid state (illustration in Figure 1), and helped by the induced electromagnetic stirring, the liquid alloy became totally homogeneous and ready to solidify in the best conditions. Cooling and solidification were carried out by decreasing voltage. After less than half an hour the obtained ingots were cold enough to be used for further preparation.

Preparation of metallographic samples; microstructure observation and hardness

The obtained ingots were cut in several parts, one thereafter serving as metallography sample and another one for preparing an electrode. Cutting was achieved using a metallographic saw. The part devoted to characterization by microscopy was placed in a plastic mold in which it was immersed by pouring a {resin + hardener} liquid mix prepared using specific products coming from ESCIL (France). After about two hours of exposure in a oven rated at 40°C, the mixture was rigidified enough to allow the

extraction out of the mold. The side with emerging metal was thus ground using abrasive papers with grade varying from #240 (coarse abrasive SiC grains) to #2400 (fine grains). After careful cleaning, the samples were polished with textile disks containing 1µm hard particles to obtain a mirror-like state. They were ready to microscopy examinations. These ones were done using a Scanning Electron Microscope (SEM; JEOL JSM-6010LA), in the Back Scattered Electrons mode (acceleration voltage: 20kV), to confirm the expected single-phased state of these alloys or to reveal any possible double-phased structure, and also to detect eventual heterogeneities in chemical composition. At the same time, the Energy Dispersive Spectrometry (EDS) device attached to the SEM allowed measuring the global chemical composition of the alloys, in order to check whether the wished compositions are well obtained. The purpose of the EDS analyses was also to confirm the total absence of other elements than cobalt and chromium.

The same metallography samples were also used to measure the hardness of the alloys. At least five indentations were carried out, according to the Vickers method. The apparatus was a Testwell Wolpert machine and the applied load was 10kg.

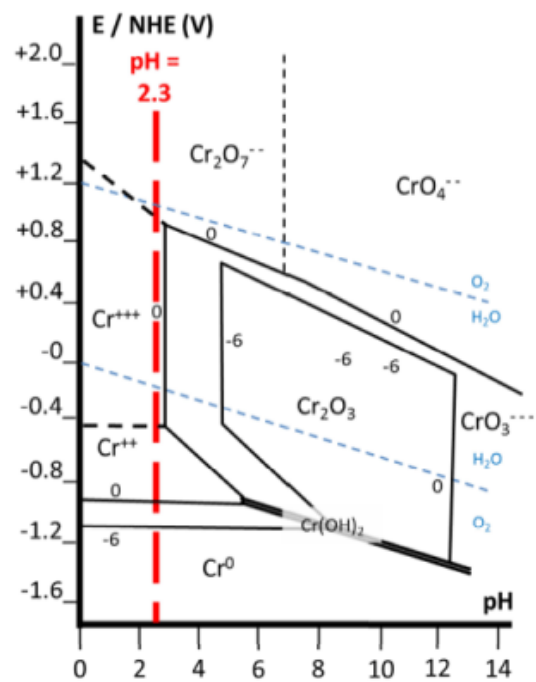


Figure 3: Simplified Pourbaix diagram of chromium

Preparation of the electrodes and of the electrolyte simulating saliva

Another part of each alloy was destined to the manufacture of the electrode. It was subjected to the same preparation as the metallographic sample but with one difference: the joining of the upper part of the metallic sample with the denuded extremity of an electric wire (copper sheathed by plastic) before pouring the {resin & hardener}-mixture in the mold (with total immersion of the {sample-copper wire}-junction. After total stiffening the side where the metallic sample appears was subjected to the same grinding and polishing sequences as the metallographic sample.

In parallel an aqueous solution was prepared to play the role of an electrolyte simulating the composition and aggressiveness of human saliva. The chemical products used to prepare it, and the concentrations with which they are introduced are presented in Table 1. This artificial saliva, of the Fusayama type, was acidified by adding diluted HCl until reaching pH=2.3. The solution was heated in a beaker placed on a hotplate while a magnetic stirrer was rotating to homogenize the solution, thermally as well as in term of dissolved oxygen. The solution was maintained at 39±1°C with the pH rated to 2.3 and the rotating magnetic stirrer during half an hour. Thereafter the solution was carefully poured in the three-electrodes cell pre-heated at 38°C, where its temperature will shortly stabilize at 37±0.5°C.

Devices used for the corrosion tests; parameters of the electrochemical tests

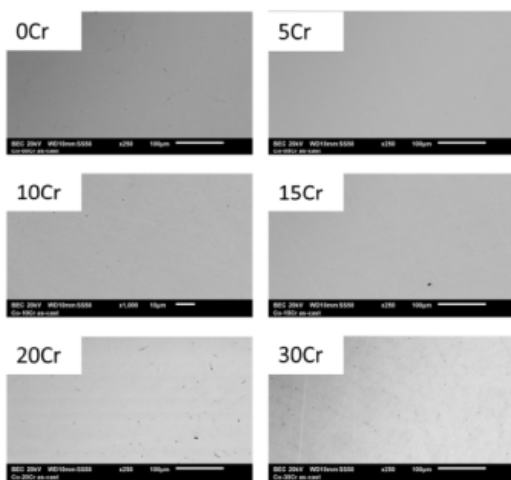


Figure 4: Microstructures of six out of the seven cobalt-based materials under study.

Table 2: Chemical composition of the elaborated alloys as specified by full frame EDS analysis.

Targeted Cr contents (wt.%)	x=5	x=10	x=15	x=20	x=25	x=30
Obtained Cr contents (wt.%)	5.2	10.5	15.5	21.6	25.6	30.8

The electrochemical cell which was used was composed of double-walled glass. Water maintained at 38°C by a thermo-cryostat F32 (JULABO) was continuously circulating through this water jacket, to allow the electrolyte of study staying at 37°C (regularly controlled using a thermometer all along the experiments). The three electrodes were:

- Working electrode: the sample of cobalt-chromium alloy embedded and polished connected to its electrical wire (it was polished again just before immersion)
- Counter electrode: platinum disk to which the working electrode was parallel (about 5 millimeters between the two, to minimize the participation of the electric resistance of the electrolyte); the current lines through the electrolyte, were thus perpendicular to both surfaces and all parallel to one another
- Reference electrode (Calomel type: +242mV / Normal Hydrogen Electrode, "NHE") placed not far from the two previous electrodes (but not in the current lines).

The potentiostat which was used was a 263A model one (EG&G/Princeton Applied Research), driven by the Powersuite software.

The electrochemical tests/measurements were of three types. First, just after immersion of the working electrode (with verification that no air bubble was trapped on surface) a one hour - stage without any electrochemical solicitation from the potentiostat was respected, to allow the establishment of the equilibrium of the whole cell (electrodes and electrolyte). The single role of the potentiostat was measuring and recording continuously the potential of the working electrode

Table 3: The two successive values of the polarization resistance acquired during the two hours of immersion before Tafel experiment

Alloys	x=0	x=5	x=10	x=15	x=20	x=25	x=30
Rp1 (Ω×cm²)	935	905	889	777	17544	170353	379462
Rp2 (Ω×cm²)	1193	871	916	967	14115	278303	565805

versus the Calomel electrode. After this first hour a first Stern Geary experiment was carried out, by polarizing the working electrode 20mV below the current free potential and applying a progressively linearly increasing potential at 10mV/min during 4 minutes. This was followed by a second 1 hour – following of free potential, itself finished with a second Stern-Geary experiment identical to the first one. Thereafter, after an intermediate stage of 5 minutes to allow new equilibrium prior to the final Tafel experiment, the working electrode was polarized at 250mV below the current free potential. The potentiostat applied a progressive linear increase in potential of a 500mV amplitude, with the constant rate of +10 mV/min.

The purposes of these measurements are to know how the free potential – or open circuit potential – E_{ocp} evolves when the alloy is in equilibrium with the electrolyte (is the alloy in active state? passivating? in passive state?). $E_{ocp}(t)$ is destined to be placed in the Pourbaix diagrams of cobalt (Figure 2 and 3) and of chromium (Figure 4). The Stern-Geary runs aim to assess the polarization resistance R_p (estimation of the corrosion rate) while the objective of the Tafel experiment is to specify more accurately the current density of corrosion I_{corr} as well as the corrosion potential E_{corr} .

Results

The obtained alloys: chemical composition, microstructure and hardness

All the alloys were successfully elaborated regardless to the chromium proportion. The obtained ingots were cut and prepared as samples ready to metallography characterization. Their chemical compositions were first specified by full frame EDS analysis. The results presented in Table 2 suggest that the wished Cr contents were really obtained in all cases.

Viewing their microstructures in Back Scattered Electrons mode allowed seeing that the alloys are seemingly all perfectly single-phased and verifying that they are also chemically homogeneous.

The indentation tests which were carried out according to the Vickers method led to the results graphically presented in Figure 5. Obviously, the progressive enrichment in chromium induced a regular increase in hardness from the around 140 Hv_{10kg} of pure cobalt to about 250 Hv_{10kg} , this demonstrating that, before a probable second effect on the corrosion resistance, the chromium content influences the

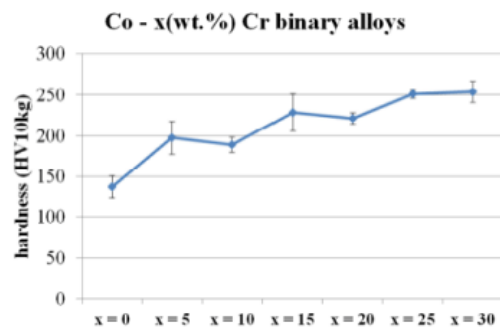


Figure 5: Vickers hardness of the studied alloys versus their Cr weight content (load: 10kg, 5 indentations per alloy)

room temperature mechanical properties.

Electrochemical results during the free immersion

First, looking to the initial levels of free potential adopted by the alloys just after their immersion in the electrolyte and to the evolution of this potential during the two first hours of immersion, gives informative view of the behaviors of the alloys. The curves of free potential evolution plotted in Figure 6 shows that, after transient high values, E_{ocp} rapidly decreases to more or less low level, which obviously depends on the Cr content in alloy. Thereafter E_{ocp} progressively rises (“xCr tf E1” part of the curves, “1” meaning the first immersion hour) and stabilizes at a level more or less 50 mV higher the reached minimum. Except for the “20Cr

alloy (the Co(bal.)-20wt.%Cr one) which shows a curious behavior; the stabilized E_{ocp} potential (end of the “xCr tf E2” part of the curves, close to the end of the second immersion hour), is dependent on the Cr content. By raising from 0 to 10-15 wt.%Cr the E_{ocp} value after 2 hours of immersion decreases and after, by raising from 15 to 30 wt.%Cr, this value of E_{ocp} significantly increases.

Regardless the alloy, the variation amplitude of E_{ocp} stays in the corrosion domain of both Cr (“Cr²⁺”) and Co

Table 4: Results of the analysis of the Tafel experiments carried out for all alloys.

Alloy	b_c (mV/dec.)	b_a (mV/dec.)	E_{corr} (mV/NHE)	J_{corr} ($\mu A/cm^2$)
0	342	36	-38	16
5	449	55	-35	27
10	449	79	-82	30
15	302	51	-64	22
20	121	332	-79	10
25	45	335	-115	0.095
30	99	155	34	0.017

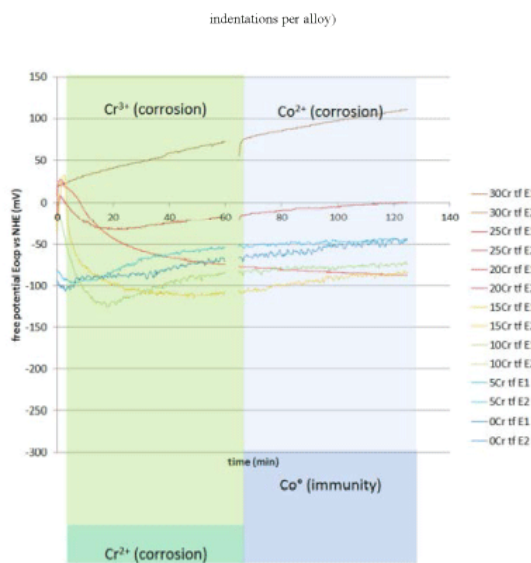


Figure 6: Evolution with time of the corrosion potential of all alloys during the 2 hours of immersion before Tafel experiment

("Co²⁺"), this suggesting that all alloys stay in an active state.

Stern-Geary results

The voids existing for all the curves correspond to the four minutes spent to apply the Stern-Geary polarization, from $E_{ocp} - 20\text{ mV}$ to $E_{ocp} + 20\text{ mV}$ with the 10 mV/min linear rate.

The slopes of these more or less linear short polarization curves allowed deducing the value of polarization resistances displayed in Table 3. Rather low Rp values were obtained after 1 hour of immersion ("Rp1") and after 2 hours of immersion ("Rp2") for the alloys containing up to 15 wt.%Cr (around $1\text{ k}\Omega \times \text{cm}^2$). In contrast they are much higher for greater Cr contents (about 200 to $500\text{ k}\Omega \times \text{cm}^2$ for 25 and 30 wt.%Cr). The Rp values obtained

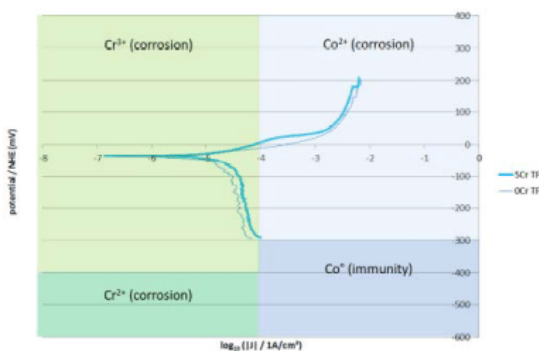


Figure 7: Tafel plots for the two Cr-lowest alloys (pure Co and Co-5 wt.%Cr)

for the "20Cr" alloy (around $15\text{ k}\Omega \times \text{cm}^2$), intermediate of these two levels, seems marking a transition, between alloys in active states (suggested by the Rp of $1\text{ k}\Omega \times \text{cm}^2$) and alloys in passive state (several hundreds of $\text{k}\Omega \times \text{cm}^2$).

Tafel runs: qualitative results

At the end of the first 2 hours of immersion a Tafel experiment was carried out for each alloy. The obtained curves are presented in Figure 7 ("0Cr" or pure Co, and "5Cr"), in Figure 8 ("10Cr", "15Cr" and "20Cr") and in Figure 9 ("25Cr" and "30Cr").

The Tafel curves of the two alloys which are the poorest in chromium are very similar to one another (Figure 10). Their cathodic part suggest a lack of dependence of the cathodic current on the applied cathodic potential, suggesting a limitation of the diffusion of the oxidant species of the solution involved in the cathodic reaction. In contrast, the anodic parts of the curves show a strong acceleration of the anodic current when the anodic applied potential increases from the potential separating the cathodic part and the anodic part (E_{corr}), before to significantly slow down.

The curves obtained for the alloys with intermediate Cr contents, which are gathered in Figure 10, are more complex, mainly in their anodic parts. The E_{corr} potentials are of the same level as the ones of the two previous alloys. But when potential moves away by higher values, the current densities increase first, then slow down, before falling to much lower values at which they seem being stabilized. This final level of anodic current observed at the highest anodic potential applied, is lower for a higher Cr content in alloy. For the Cr-richest one of the three alloys, "20Cr", the current starts to be almost undetectable and a little unstable. This type of behavior during a Tafel

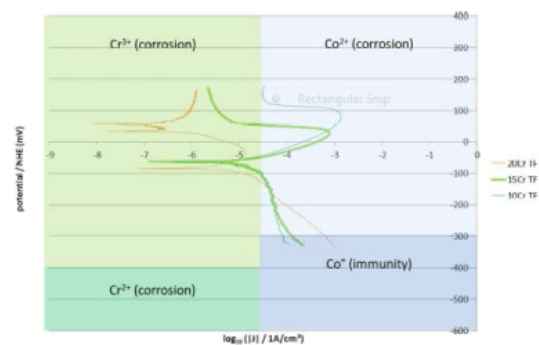


Figure 8: Tafel plots for the three medium Cr alloys (Co-10, 15 and 20 wt.%Cr)

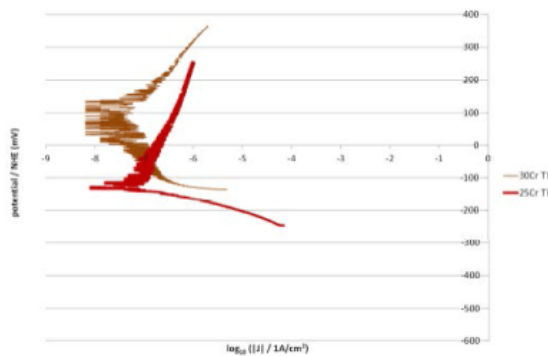


Figure 9: Tafel plots for the two Cr-richest alloys (Co-25 and 30 wt.%Cr)

experiment suggests a passivation phenomenon in the anodic part of the curve, validated by the particularly lowered values of the anodic currents observed at the highest applied potential. Consequently this demonstrate that before, the alloys were still in an active state.

By comparison with the five previous Tafel curves, the ones obtained for the two Cr-richest alloys, “25Cr” and ‘30Cr”, are shifted on the left, as is to say to extremely low values of current densities, for the cathodic parts as well as for the anodic parts. At the same time, the parts of Tafel curves which are close to the E_{corr} values are particularly noisy, because the lack of accuracy of the potentiostat for measuring so low currents. This is characteristic of passivated alloys.

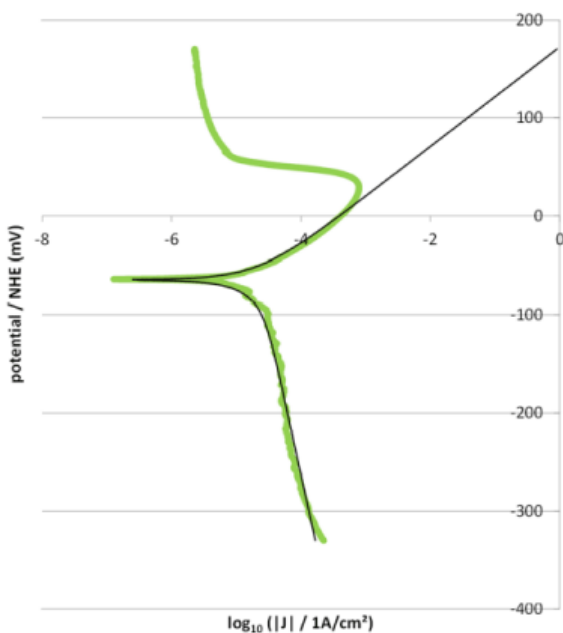


Figure 9: Tafel plots for the two Cr-richest alloys (Co-25 and 30 wt.%Cr)

Tafel runs: quantitative results

The purpose of Tafel experiment is basically to numerically analyze the obtained $I=f(E)$ curves in order to specify J_{corr} with a much better accuracy than with Stern-Geary (from the R_p values). At the same time the values of E_{corr} and of the two Tafel coefficients (the cathodic one (b_c) and the anodic one (b_a)) can be obtained in parallel. Tafel analysis was carried out for all the obtained Tafel curves, and validated by comparison between the theoretic Tafel curve mathematically drawn using the obtained values (according to the Butler-Volmer equation) and the original experimental curve. An example of such validation of the values obtained for E_{corr} , J_{corr} , b_a and b_c is given in Figure 10. In this illustration, the mathematical curve (black fine) plotted with the results of Tafel analysis of the experimental curve (thick green), is well fitting the later one for the part acquired before passivation happened.

The values of E_{corr} , J_{corr} , b_a and b_c obtained and validated, are presented in Table 4. One can see that the cathodic Tafel coefficient (b_c) is around 400 mV / decade for the alloys with 15 wt.%Cr or less, against about one hundred of mV / decade for the three Cr-richest alloys. The order is inverted for the anodic coefficient: b_a is lower (< 100 mV / decade) for the four Cr-poorest alloys than for the three Cr-richest ones (> 150 mV / decade). No systematic evolution of the corrosion potential can be noted, contrarily with what clearly appears for the current densities: the alloys containing less than 20 wt.%Cr corrode rather rapidly (several tens of $\mu A / cm^2$) while the corrosion current falls down to only 100 nA/cm² and less as soon as the Cr content reaches and exceeds 25 wt.%Cr.

Discussion

The first observation done in this work was that none of the seven alloys was problematic to synthesize. The 50 kW high frequency induction furnace which was involved for that was powerful enough to melt cobalt and chromium regardless to the relative proportions of these elements. One can think that if novel chromium content should be chosen instead the commonly chosen contents this ought to do not induce elaboration problems for manufacturers. However, before considering the {Cr content ↔ corrosion behavior} relationships, care must be taken concerning the consequences of the Cr content on the hardness, and more generally on the mechanical properties.

Concerning the behavior of these alloys in corrosion, it may be legitimate to be initially a little anxious, by

considering first the standard potentials of the redox couples concerned by these binary alloys. Indeed, at pH=0, $E^0(\text{Co}^{2+}/\text{Co}^0) = -0.28 \text{ V}$, and even worse: $E^0(\text{Cr}^{2+}/\text{Cr}^0) = -0.91 \text{ V}$, the first one just a little higher than the standard potential of $\text{Fe}^{2+}/\text{Fe}^0$ (-0.44 V) and the second one, significantly lower than this later value. Knowing the almost catastrophic behavior of pure iron in acidic solutions, one can guess that possible problems of rapid corrosion of some of the alloys considered in this study may occur.

However, by reminding how ferritic (Fe-Cr-C) or austenitic (Fe-Ni-Cr-C or Fe-Ni-Cr-Mo-C, e.g. AISI 304 and AISI 316) stainless steels resist against corrosion, even in acidic milieus, one may be initially reasonably optimistic for the Cr-richest cobalt alloys. Indeed, even if the pH rated for the artificial saliva was too low to allow protection of the alloys thanks to a passivation phenomenon resulting from the development of a thin scale of cobalt or chromium hydroxides, as shown by the E-pH diagrams reminded in Figures 3-4, local high cationic concentration can result in the precipitation of such solids ($\text{Co}(\text{OH})_2/\text{CoO}$, $\text{Cr}(\text{OH})_3/\text{Cr}_2\text{O}_3$), the second species being the much more probable ones.

The characterization of the behaviors in the present acidified artificial saliva of all the considered cobalt alloys was necessary to clarify the situation, anyway. Obtaining really homogeneous alloys after casting was particularly favorable to a better characterization and a better understanding of the phenomena. Indeed, the addition of multiple contributions from the different phases existing in a multiphased alloy, and simply also the added contributions from different chemically different zones of a same phase because of chemical segregation during solid growth, may lead to a global and unique signal, in term of current density as well as of potential. In the case of the seven alloys studied here, the single possible heterogeneity is at the grains / grain boundaries level. This limited the dispersion of results (except in some rare cases (e.g. the "20Cr" alloy) and rather clear conclusions were possible to do.

This first concerned the E_{ocp} potentials. The average level of E_{ocp} potential was either low (alloys with Cr contents from 0 to 15 wt.%) or high (Co - 25 or 30 wt.%). In the first case it is natural to think that the alloys were in an active state, with the absence of any continuous oxide/hydroxide layer separating the metallic alloys and the electrolyte. E_{ocp} is not constant but it stays in the corrosion domains

of Co and Cr (domains of Co^{2+} and Cr^{3+} predominance). It is defined by the equilibrium between, one the first hand the cathodic currents associated to the reduction of protons and dissolved oxygen ($\text{H}^+ + \text{e} \rightarrow \frac{1}{2} \text{H}$ and $\frac{1}{2} \text{O} + \text{H}^+ + 2 \text{e} \rightarrow \text{OH}^-$), of the other hand the anodic currents resulting of the oxidation of Co ($\text{Co} \rightarrow \text{Co}^{2+} + 2 \text{e}$) and Cr ($\text{Cr} \rightarrow \text{Cr}^{3+} + 3 \text{e}$). In the second case the same cathodic reactions are balanced by only the extremely low oxidation of Co and/or Cr through the protective $\text{Cr}(\text{OH})_3$ or Cr_2O_3 passivation scale. Obviously, its intermediate Cr content does not allow the Co - 20 wt.%Cr alloy definitely passive all along the two first hours of immersion. This is confirmed by the obtained polarization resistances (Table 3) which are 300 times higher for the "25Cr" and "30Cr" alloys (suggesting corrosion currents 300 times lower) than for the alloys poor in chromium (up to 15 wt.%).

The richer information brought by the Tafel runs themselves confirm these behaviors by clearly demonstrating the nature of the corrosion states of the alloys. The more useful Tafel curves to start explaining that are the ones presented in Figure 8. Their cathodic parts are typical of an active state, as well as the beginning of the anodic part. After about 100 to 150 mV increase from E_{corr} , the anodic current still rises but decelerates to finally stay

(maximum of current in the anodic peak) before more or less abruptly falling. This more or less progressive fall in anodic current density is due to the more or less fast development of a passivation layer. By considering the necessary amplitude of potential increase from E_{corr} and the height in current density of the anodic peak counted from J_{corr} , it is clear that the higher the Cr content in the alloy, the easier the passivation phenomenon: the "20Cr" alloy passives sooner (at +70 mV / E_{corr} against +150 mV / E_{corr}) and easier (anodic peak at less than 10 $\mu\text{A}/\text{cm}^2$ against less than a little less than 1 mA/cm^2) than the "15Cr" alloy the passivation of which is itself sooner (at +150 mV / E_{corr} against +200 mV / E_{corr}) and a little easier (anodic peak at a little less than 1 mA/cm^2 against a little more 1 mA/cm^2) than the "10Cr" alloy. Furthermore, the higher the chromium content the thicker and the more protective the passivation layer: the anodic current in the passivation plateau of the "20Cr" alloy is about 1 $\mu\text{A}/\text{cm}^2$, against about 5 $\mu\text{A}/\text{cm}^2$ for the "15Cr" alloy and 20 $\mu\text{A}/\text{cm}^2$ for the "10Cr" alloy.

By comparison the two Cr-poorest alloys ("0Cr" and "15Cr") did not succeed in passivating (Figure 7) while

the two Cr-richest alloys ("25Cr" and "30Cr") were obviously already passivated when they underwent the Tafel experiments, with absence of any anodic peak but extremely low anodic currents (and of course values of J_{corr} order of magnitude: $0.1 \mu\text{A} / \text{cm}^2$).

The values of E_{corr} , J_{corr} and of the two Tafel coefficients, determined by Tafel analysis the seven curves, were displayed in Table 4. The typical value of J_{corr} for the alloys not able to passivate and therefore remaining in active state all the time is about $20 \mu\text{A} / \text{cm}^2$. By considering the reaction of oxidation of Co (in Co^{2+}) and of Cr (in Cr^{3+}), these $20 \mu\text{A} / \text{cm}^2$ correspond to $1/n \times (J_{\text{corr}} / F) = 1/n \times (20 \times 10^{-6} \text{ C s}^{-1} \text{ cm}^2 / 96500 \text{ C mol}^{-1}) \times 3600 \text{ s h}^{-1}$, as is to say a release of $0.37 \mu\text{mol/h/cm}^2$ of Co^{2+} cations ($n = 2$) and $0.25 \mu\text{mol/h/cm}^2$ of Cr^{3+} cations ($n = 3$). So, if one considers 1 cm^2 of total framework surface exposed to saliva and 10 cm^3 of saliva present in mouth, an active state would lead to an increase of about $3 \times 10^{-5} \text{ mol/L}$ more per hour of a mix of Co^{2+} and Cr^{3+} anions in mouth. This remains to be compared to allowable concentration values but one can guess now that an active state is not tolerable. The J_{corr} values in the passive state (alloys with 25 to 30 wt.%Cr), which are one thousand times lower, correspond to a production of only $0.03 \mu\text{mol} / \text{L} / \text{h}$ much lower than the preceding values. Furthermore, in their cases, it is very possible that the J_{corr} corresponds only to the slow thickening of the passivation layer (production of $\text{Cr}(\text{OH})_3$ or Cr_2O_3 only, not of cations). This can be verified by very long immersion tests of these alloys followed by analysis of the solution.

For the moment, the observed behaviors of the studied alloys allow understanding why the Cr content in commercial {cobalt, chromium}-based alloys are generally rated at 25 wt.% Cr or little higher [21-23].

Conclusion

The chromium content is a key factor in the corrosion behavior of Predominantly Base dental alloys, regardless to the base element, nickel or cobalt. This is the passivation layer the development of which it favors, in which it is involved, that allows these cheap alloys competing with alloys rich in noble metals. Its content must be carefully rated to avoid either perfectible protection (not total passivation, risk of loss of the passive state... if content not high enough) or casting difficulties and ambient temperature brittleness (Cr oxidation during heating, first

melting from pure elements, loss of ductility due to Co-Cr sigma phases...).

To allow credible comparisons between alloys containing Cr with rather neighbor contents to accurately choose an optimized content, as done here with rather fine slices in Cr content (of 5 wt.%Cr), the procedure needed to be very stabilized over all parameters. This is what was done here with notably: single-phased alloys really homogeneous in Cr content all over the electrode surface, with the mechanical state (same protocol of post-solidification cooling, cutting, grinding/polishing... as is to say the same residual stresses and hardening state for all alloys)... Despite this very careful procedure, minor discrepancies staid possible. However the identification of a minimal Cr content (25wt.% Cr) was successfully done.

Acknowledgments

The authors wish thanking sincerely Mr. Thierry Schweitzer for his technical help in this work.

References

1. De March P. Etude électrochimique et métallographique des alliages et brasures utilisés en prothèse fixée dentaire céramo-métallique. PhD Thesis. Nancy: University Henri Poincaré; 2011.
2. Donachie MJ, Donachie SJ. Superalloys – A technical guide. 2nd ed. Materials Park: ASM International; 2002.
3. Bradley EF. Superalloys – A technical guide. Metals Park: ASM International; 1988.
4. Kofstad P. High temperature corrosion. London: Elsevier applied science; 1988.
5. Beaufils S, Pierron P, Millet P. Allergy in the non-precious dental alloys: data of the literature and current solutions. Actual. Odonto-Stomatol. 2016; 275.
6. Wataha JC. Biocompatibility of dental casting alloy: A review. J Prosthet Dent 2000; 83(2):223-34.
7. Eliasson A, Arnelund CF, Johansson A et al. A clinical evaluation of cobalt-chromium metal-ceramic fixed partial denture and crowns: a three-to-seven-year retrospective study. J Prosthet Dent 2007; 98:6-16.
8. Hansson O; Moberg LE. Evaluation of three silicoating methods for resin-bonded prostheses. Scand J Dent Res 1993; 101(4):243-51.
9. Fredriksson H, Sunnerkrantz PA, Victorin L. A binary dental gold-cobalt alloy of eutectic composition. Acta Odontol Scand 1983; 41(3):135-41.
10. Lin JHC, Lo SJ, Ju CP. Biocorrosion study of titanium-cobalt alloys. J Oral Rehabil 1995; 22(5):331-5.

11. Ghiban A, Ghiban B, Bortun CM, Buzatu M. Structural investigations in CoCrMo(Ti) welded dental alloy. *Revista de Chimie (Bucharest, Romania)* 2014; 65(11):1314-8.
12. Mueller M, Hirschfeld D. Alloy for articles with great corrosion resistance and/or severe mechanical wear and tear. Patent Ger. Offen. (1976) DE 2511745 A1 19760923.
13. Tarcolea M, Hancu V, Miculescu F, Smatrea O, Coman C, Comaneanu RM, Ormenisan A. Research on microstructural and chemical inhomogeneity in cast metal crowns made of CoCrMoW alloy. *Revista de Chimie (Bucharest, Romania)* 2015; 66(8):1143-6.
14. Stierschneider H, Kulmburg A. Dental alloy. Eur. Pat. Appl. (1981) EP 41938 A2 19811216.
15. Matinlinna JP, Laajalehto K, Laiho T, Kangasniemi I, Lassila LVJ, Vallittu PK. Surface analysis of Co-Cr-Mo alloy and Ti substrates silanized with trialkoxysilanes and silane mixtures. *Surf Interface Anal* 2004; 36(3): 246-53.
16. Lindigkeit J. Cast dental alloy. Patent. Ger. (2003) DE 10226221 C1 20031211.
17. Weronki A. Cobalt alloy for dental and surgical purposes. Patent Pol. (1992), PL 154905 B1 19910930.
18. Podesta CE, Da Silva LM. Cobalt-chromium and nickel-chromium alloys as biomaterials for use in dentistry, orthopedics, and the automotive industry. Patent Braz. Pedido PI (2012) BR 2010002077 A2 20120313.
19. Cascone PJ, Prasad A. Method of making dental prosthesis and ductile alloys for use therein. Patent PCT Int. Appl. (2013), WO 2013155480 A1 20131017.
20. Contu F, Elsener B, Boehni H. Corrosion behaviour of CoCrMo implant alloy during fretting in bovine serum. *Corrosion Science* 2005; 47(8): 1863-75.
21. Vermilyea SG, Tamura JJ, Mills DE. Observations on nickel-free, beryllium-free alloys for fixed prostheses. *J Am Dent Assoc* 1983;106 (1):36-8.
22. Reclaru L, Lüthy H, Eschler PY, Blatter A, Sus z C. Corrosion behaviour of cobalt- chromium dental alloys doped with precious metals. *Biomaterials* 2005; 26: 4358-65.
23. Kim EC, Kim MK, Leesungbok R, Lee SW, Ahn SJ. Co-Cr dental alloys induces cytotoxicity and inflammatory responses via activation of Nrf2/antioxidant signaling pathways in human gingival fibroblasts and osteoblasts. *Dent Mater* 2016; 32:1394-1405.